Cell Metabolism, Volume *14*

Supplemental Information

In Vivo Correction of COX Deficiency by Activation of the AMPK/PGC-1α Axis

Carlo Viscomi, Emanuela Bottani, Gabriele Civiletto, Raffaele Cerutti, Maurizio Moggio, Gigliola Fagiolari, Eric A. Schon, Costanza Lamperti, and Massimo Zeviani

Inventory of Supplemental Information

Tables S1–S4 summarize the results of biochemical assays of the respiratory chain complexes I-IV and citrate synthase.

Figure S1 and legend report some of the effects of bezafibrate treatment of Surf1$^{-/-}$ and control littermates.

Figure S2 and legend report the strategy for the construction of a *Cox15* conditional knockout allele and the corresponding genotyping diagnosis in recombinant mice.

Figure S3 and legend report the effects of bezafibrate treatment in skeletal muscle of *ACTA-Cox15*$^{-/-}$ mice.

Table S1: Specific activities of citrate synthase (CS) and MRC complexes (CI-IV) in ACTA-Cox15$^{-/-}$ mice (n.3) and COX15$^{lox/lox}$ (n.3), considered as WT. Values are expressed as nanomoles/min/mg protein

	CS	**CI**	**CII***	**CIII**	**CIV*****
CTR	354.7±103.5	186.0±77.4	24.2±4.2	283.3±26.4	347.0±97.1
Cox15$^{-/-}$	487.3±84.9	248.0±77.8	35.0±7.8	314.7±41	30.7±9.2

* Student's *t* test p<0.05
*** Student's *t* test p<0.005

Table S2. Specific activities of MRC complexes CI-IV and citrate synthase (CS) of Surf1$^{-/-}$ and WT littermates. Values are expressed as nanomoles/min/mg protein

	CS	**CI**	**CII**	**CIII**	**CIV**
WT	363.3±39.2	163.3±39.7	37.9±11.5	339.9±15.5	382.5±45.2
WT AICAR	418.8±124.0	127.5±50.2	56.9±14.3	362.6±127.2	514.3±80.5*
Surf1$^{-/-}$	310.8±66.8	96.2±21.2	34.2±13.7	249.7±44.3	100.6±7.8
Surf1$^{-/-}$+AICAR	336.4±52.3	144.6±18.1*	46.1±4.4**	352.6±45.8*	161.0±3.5***

Student's *t* test *p<0.05; **p<0.01; ***p<0.001

Table S3. Specific activities of MRC complexes CI-IV and citrate synthase (CS) of Sco2^{KOKI} and WT littermates. Values are expressed as nanomoles/min/mg protein

	CS	**CI**	**CII**	**CIII**	**CIV**
WT	289.0±104.0	136.3±77.3	24.9±2.6	517.3±17.5	332.8±48.2
WT+AICAR	349.0±115.1	156.5±47.2	32.3±6.7	598.6±24.2*	350.3±36.0
Sco2^{KOKI}	408.0±55.4	88.2±16.2	34.7±13.7	206.0±41.3	172.6±49.8
Sco2^{KOKI} AICAR	546.2±123.2	134.6±26.1*	57.1±5.6*	374.6±85.8*	247.0±39.5**

Student's *t* test *p<0.05; **p<0.01

Table S4. Specific activities of MRC complexes CI-IV and citrate synthase (CS) of ACTA-Cox15$^{-/-}$ and WT littermates. Values are expressed as nanomoles/min/mg protein

	CS	**CI**	**CII**	**CIII**	**CIV**
WT	341.2±104.6	186.1±77.3	24.2±4.2	283.1±26.7	347.2±97.2
WT AICAR	349.2±115.3	156.6±47.5	32.3±6.7	471.4±27.3**	768.2±17.2**
Cox15$^{-/-}$	487.3±85.1	248.0±78.1	34.9±7.8	315.3±41.2	30.7±9.0
Cox15$^{-/-}$+AICAR	661.1±9.1	237.6±10.2	46.0±17.6*	549.3±86.1**	127.5±15.4***

Student's *t* test *p<0.05; **p<0.01; ***p<0.001

Figure S1
Bezafibrate treatment in Surf1$^{-/-}$ mice.
A: body weight during treatment. Red lines: Surf1$^{-/-}$ mice (n. 3). Blue lines: WT littermates (n. 3). Continuous lines: untreated animals. Dotted lines: treated animals (seet main text for details).
B: liver enlargement at autopsy of a treated vs. an untreated Surf1$^{-/-}$ mice.
C: liver weight/body weight in untreated (Unt) vs. treated (bzf) animals (n. 3 for each group).

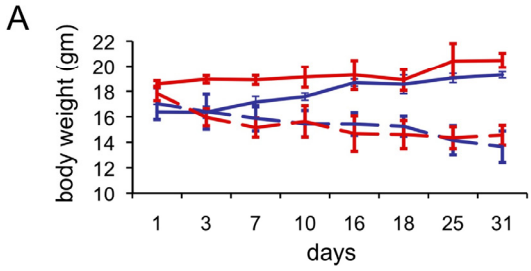

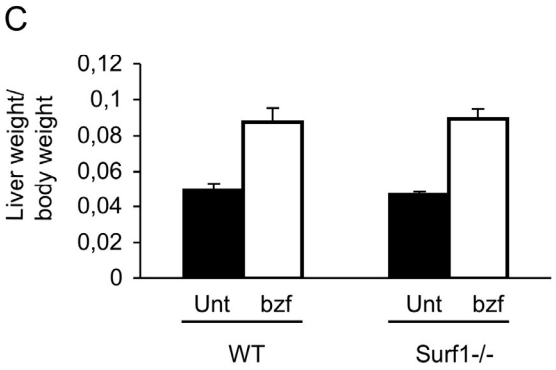

Figure S2

Cox15^{lox} and ACTA-Cox15$^{-/-}$ recombinant alleles

A. Schematic structure of wild type (WT) and recombinant Cox15^{lox} allele. Short and long arm of homology are shown in blue. A neomycin-resistance cassette is shown in yellow. Two lox-P sites are located in introns flanking exons 1 and 2. Arrowheads indicate the position of primers used specific to the short arm (SA1/F and Neo/R) and the long arm (Neo/F and LA1/R) for the screening of recombinant ES cells. Note that both SA1/F and LA1/R are located in regions outside the recombinant construct. Primer sequences are available on request.

B. PCR-based screening of positive ES clones using the primer pairs SA1/F and Neo/R (left panel) specific for the short arm, and Neo/F and LA1/R (right panel) specific for the long arm. Clone 4 shows the expected fragments at 3.2kb (short arm) and 9.8 kb (long arm). Positive (+) and negative (-) controls are shown, as well as four non-recombinant clones (1, 2, 3, 5).

C. Left: schematic structure of the recombinant Cox15^{lox} allele before (top) and after (bottom) cre-mediated recombination of the region encompassed by the two lox-P sites. Arrowheads indicate the position of the primer pairs Cox15lox/F and Cox15lox/R used for the genotype analysis. Right: PCR-based genotyping in muscle (M), heart (H), liver (L) and brain (B) of Cox15$^{lox/lox}$ vs ACTA-Cox15$^{-/-}$ alleles of two recombinant animals. Note that the diagnostic band specific to the ACTA-Cox15$^{-/-}$ allele is present only in skeletal muscle and, in trace amount, in the heart.

Primer sequences are available on request.

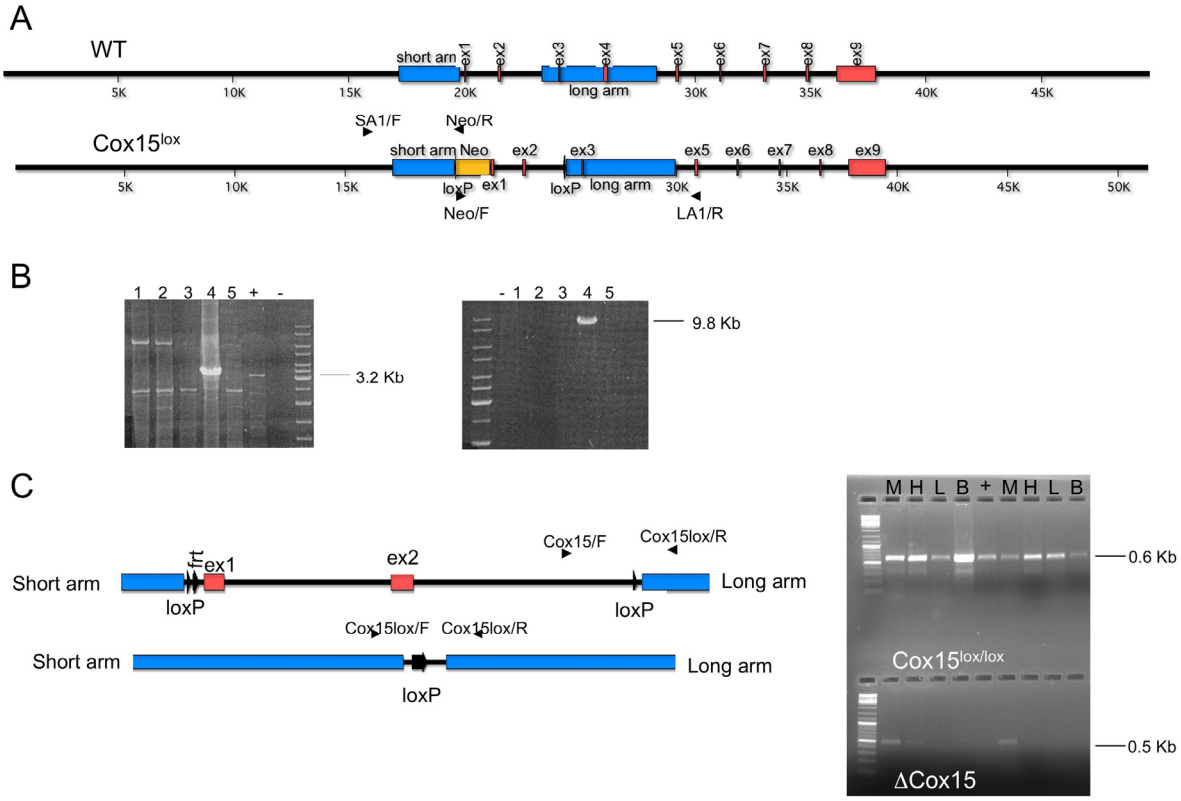

Figure S3
Effects of bezafibrate of *ACTA-Cox15*$^{-/-}$ *mice*

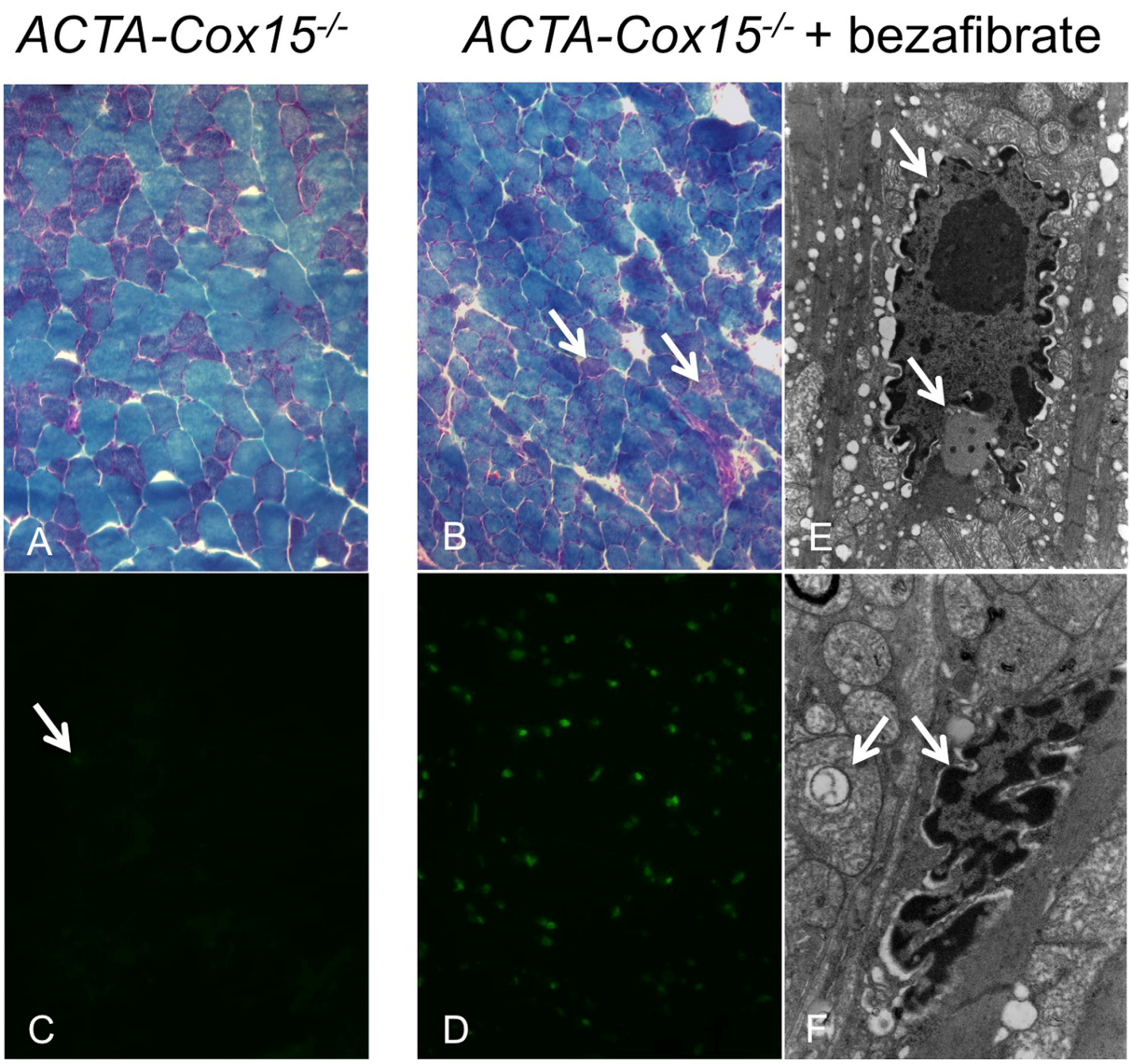

Gomori trichrome staining of muscle from A) an *ACTA-Cox15*$^{-/-}$untreated mouse (*panel A*) and bezafibrate-treated *ACTA-Cox15*$^{-/-}$ mouse (*panel B*). Note the increase of ragged-red fibers, fiber-size variation and central nuclei in the bezafibrate-treated muscle. Arrows indicate two degenerated fibers. Magnification 20x.
TUNEL staining in sections serial to those shown in *panels A* and *B*. The bezafibrate-treated muscle (*panel D*) contains numerous TUNEL-positive fluorescent green nuclei, compared to a single weakly TUNEL-positive nucleus present in untreated muscle, indicated by an arrow (*panel C*).
Panel E: Electron microscopy (EM) of a nucleus in a muscle fiber from a bezafibrate-treated *ACTA-Cox15*$^{-/-}$ mouse. Note the gaps in the nuclear membrane and an apoptotic body (arrows). Magnification 20000x.
Panel F: EM of a piknotic nucleus and a vacuolated mitochondrion (arrows) in a muscle fiber from a bezafibrate-treated *ACTA-Cox15*$^{-/-}$ mouse. Magnification 20000x.